**Atmospheric
Chemistry
and Physics
Discussions**

Weather response to management of a large wind turbine array

D. B. Barrie and D. B. Kirk-Davidoff

Department of Atmospheric and Oceanic Science, University of Maryland, College Park, MD, USA

Correspondence to: D. B. Barrie (dbarrie@atmos.umd.edu)

ACPD

9, 2917–2931, 2009

Weather response of a large wind turbine array

D. B. Barrie and
D. B. Kirk-Davidoff

Title Page

Abstract	Introduction
Conclusions	References
Tables	Figures

|◄ | ►|

◄ | ►

Back | Close

Full Screen / Esc

Printer-friendly Version

Interactive Discussion

Abstract

Electrical generation by wind turbines is increasing rapidly, and has been projected to satisfy 15% of world electric demand by 2030. The extensive installation of wind farms would alter surface roughness and significantly impact the atmospheric circulation, due to the additional surface roughness forcing. This forcing could be changed deliberately by adjusting the attitude of the turbine blades with respect to the wind. Using a General Circulation Model (GCM), we represent a continent-scale wind farm as a distributed array of surface roughness elements. Here we show that initial disturbances caused by a step change in roughness grow within four and a half days such that the flow is altered at synoptic scales. The growth rate of the induced perturbations is largest in regions of high atmospheric instability. For a roughness change imposed over North America, the induced perturbations involve substantial changes in the track and development of cyclones over the North Atlantic, and the magnitude of the perturbations rises above the level of forecast uncertainty.

1 Introduction

The development of numerical weather prediction (NWP) by John von Neumann and Jule Charney was motivated in part from a desire to influence weather at a distance (Kwa, 2002). However, von Neumann recognized that the practical means to exert control on large-scale weather did not yet exist (Kwa, 2002). While NWP was being developed, Irving Langmuir and Vincent Schaefer's work on cloud seeding provided an early method for manipulating precipitating systems (Langmuir, 1950; Schaefer, 1946). Langmuir (1950) suggested that cloud seeding could be used to suppress hurricanes by altering early convective growth in tropical disturbances. However, in subsequent attempts at cyclonic-scale modification such as Project Stormfury, investigators did not have at their disposal either the ability to introduce perturbations in the circulation larger than the observational uncertainty, or knowledge of the error growth mode structure

sufficient to match the perturbations to the growing modes (Willoughby et al., 1985).

The chaotic growth of small initial perturbations in the atmosphere (Lorenz, 1963) has both positive and negative implications for weather modification strategies. A small perturbation in the atmosphere may eventually become large enough to have detectable consequences for weather. However, chaos limits weather predictability to a few weeks, since the various atmospheric states consistent with observational uncertainty diverge completely from one another over that time (Lorenz, 1969). Thus, deliberate synoptic scale weather modification requires the ability to introduce perturbations that are larger than observational uncertainty. These perturbations must also project onto atmospheric modes with the potential to grow in a desired direction. Hoffman (2002) proposed a program of global weather modification in which weather would be optimized by systematically adjusting all human controlled phenomena that could influence the atmosphere's flow. Hoffman et al. (2006) demonstrated in a model that hurricanes could be steered by creating an ideal initial perturbation in the temperature field. However, the introduction of that perturbation required impractically large energy inputs.

Previous modeling studies have shown that significant mean changes in climate patterns result from the introduction of large-scale wind farms (Kirk-Davidoff and Keith, 2008). Effects on meteorology have also been demonstrated for wind farms of a smaller size in a regional model (Baidya Roy et al., 2004). These findings suggest that a step change in the effective roughness of a large-scale wind farm might introduce a perturbation in the atmospheric flow larger than the observational uncertainty. In this study, we examine the evolution of perturbations caused by such step changes in a fixed array of wind turbines within a synoptic forecast period. The continental scale of this wind farm is consonant with that of growing synoptic-scale modes, and the amplitude of the roughness forcing is large when compared with the typical background observational uncertainty of the mean wind in model initializations at the National Center for Environmental Prediction. Although synoptic-scale perturbations grow slowly relative to convective-scale perturbations (Schubert and Suarez, 1989), they saturate at higher

Weather response of a large wind turbine array

D. B. Barrie and
D. B. Kirk-Davidoff

◄◄ | ►►

◄ | ►

Back | Close

Full Screen / Esc

Printer-friendly Version

Interactive Discussion

amplitudes than convective modes (Toth and Kalnay, 1993), suggesting that weather modification may be possible by taking advantage of the short-term predictability of mid-latitude instabilities. While large-scale wind turbine installations like those discussed in this paper do not yet exist, no known resource limitations would prevent their construction in the near future.

1.1 The potential for large-scale wind farms

The worldwide wind energy potential has been assessed at 72 Terawatts (TW) (Archer and Jacobson, 2005). Total worldwide electric power consumption is projected to nearly double from 1.9 to 3.5 TW between 2004 and 2030 (Dorman et al., 2007). A large contribution from wind energy is typically proposed when modeling the power supply system under carbon constraints (e.g. Aubrey et al., 2006; Department of Energy, 2008; Pacala and Socolow, 2004). Continued rapid growth of the United States wind industry will result in substantial development of its wind resource. The Central United States will be a focal point of this development because it hosts the largest contiguous wind resource of any on-shore region in the United States (Elliott et al., 1986). Turbine installation costs are lower there than in any other region of the United States (Wiser and Bolinger, 2004). In addition, wind farm developers are willing to pay leasing fees to farmers for the use of their land to build wind farms, resulting in a substantial source of supplemental income for farmers in the Midwestern United States (Department of Energy, 2004).

2 Model description

Individual wind turbines affect local momentum transports through the creation of a cross-blade pressure gradient and turbulent wakes (Medici, 2004). The aggregate impact of an array of wind turbines can be parameterized by a single roughness length (Vermeer et al., 2003). This is the approach we have taken using the National Center

Weather response of a large wind turbine array

D. B. Barrie and
D. B. Kirk-Davidoff

for Atmospheric Research Community Atmosphere Model 3.0 (CAM 3.0) (Collins et al., 2006).

2.1 Wind farms as a surface roughness length

CAM 3.0 describes land surface characteristics using the spatial and temporal distribution of 16 Plant Functional Types (PFTs) across the land surface. Each land gridpoint can support four unique PFTs, with coverage adding up to 100% over each grid point (Barlage and Zeng, 2004). We have converted an unused PFT into a wind farm subtype, with a "canopy" height of 156 m (to simulate wind turbines with 100 m towers and 56 m blades), a ratio of roughness length to canopy height of 0.0215, and a displacement height of zero meters. Wind turbine roughness length was calculated using the Lettau method (Lettau, 1969), assuming turbine spacing of 3.4 blade diameters. This low value of turbine spacing was used because the wind farm PFT was set to occupy only 25% of the surface area within the wind farm region. This reduces the areal coverage of the wind farm PFT, and thus the packing density of the wind turbines.

2.2 Model runs

The model was run with fixed sea surface temperatures at T42 resolution for six years with the wind farm present. The wind farm occupies 23% of the North American land area and is positioned in the central United States and south central Canada. Seventy-two case studies were created by running the model in branch mode using the monthly restart files created during the six years of the control run. Each of the branch runs lasted for one month. For these case studies, the wind farm PFT roughness was reduced by 83% to simulate the minimal drag of a turbine profile, where the face of the turbine is turned so that it is orthogonal to the wind direction. The branch runs simulate the effect of a sudden, large reduction in surface roughness on the atmosphere.

One case study was examined in detail to determine the extent to which the observed atmospheric perturbations are sensitive to initial conditions. Five sets of initial

conditions were created by adding to the temperature field a normally distributed random perturbation with a standard deviation equal to 1% of the standard deviation of the temperature field, to represent observational uncertainty in the initial conditions for the forecast.

5 ## 2.3 Dissipation due to surface roughness

Using 12-hourly lowest model level winds (corresponding to an altitude of approximately 80 m) and the turbine parameters discussed in Sect. 2.1, we derived a total maximum energy output for our hypothetical wind farm of 2.48 TW. This is the power that would be produced if perfectly efficient turbines of unlimited nameplate capacity
10 were installed over the entire region.

Power dissipation in the wind farm region was calculated to be, on average, 9.66 TW. This calculation used wind and surface stress data. This number does not change substantially due to the presence or absence of the turbines, since it is constrained by the import of momentum into the region by the large-scale flow. Instead, the model
15 atmosphere responds to the increased roughness by reducing the wind speed over the wind farm at the lowest model level and maintaining nearly constant dissipation. We can interpret this as a shift from conversion of kinetic energy to heat via the motion of vegetation, to conversion of kinetic energy to electrical power in the wind turbine generators. At the sub-grid level of the land surface parameterization, wind stress
20 increases despite the lower mean wind over the fractional grid squares where the wind turbines are located. This occurs because the ratio between wind speed and wind stress approximately doubles, due to the twenty-fold increase in roughness length (see Eq. (4.434) in Collins et al., 2004). At the same time, wind stress over the fractional grid squares with vegetation coverage decreases due to the reduced wind speed.

25 The Lettau method, which was used for estimating the turbine roughness length, becomes increasingly inaccurate for sparsely distributed elements, such as wind turbines in a wind farm (Macdonald et al., 1998). Despite these difficulties, we have chosen to use the Lettau method because we believe it to be conservative (see Fig. 1 of Macdon-

D. B. Barrie and
D. B. Kirk-Davidoff

Title Page

Abstract	Introduction
Conclusions	References
Tables	Figures

⏮ ⏭

◀ ▶

Back Close

Full Screen / Esc

Printer-friendly Version

Interactive Discussion

ald et al. 1998). For example, Baidya Roy et al. (2004) showed that in a high vertical resolution model of a 100 km – scale wind farm, momentum was driven away from the turbine hub-height, increasing winds at the surface and above the turbine blades, and increasing surface dissipation. No standard method exists to model the impact of an array of moving objects as a roughness length; we look forward to field research that will allow more accurate representation of wind farm drag on the atmospheric flow field in large-scale models.

3 Results

Figure 1 shows the mean difference between the case and control runs in the eastward wind field at the lowest model level. The impacts are, on average, focused within the wind farm, where there is a slowing of the wind. There is also a region of zonal acceleration extending from Northern Canada to Western Europe. The rectangular outline in the figure demonstrates the placement of the wind farm. The structure of the anomaly is similar to that found in a previous 20 year model run with and without wind farm forcing, and it arises from the dynamical adjustment of the atmosphere to the surface roughness anomaly (Kirk-Davidoff and Keith, 2008).

During the first few days following the decrease in magnitude of the surface roughness perturbation in each case, we observe highly localized wind and temperature anomalies that are contained primarily within the wind farm and depend strongly on the overlying meteorological conditions. Over the following days, the impacts move downstream and eventually reach the North Atlantic. There the anomalies grow, and their magnitudes exceed the magnitude of the response at the wind farm. This is shown in Fig. 2a, a Hovmoller plot of the standard deviation over the 72 case studies. The zonal wind in the lowest model layer is depicted in the plot and was averaged over the band from 29 to 57° N to capture the effects directly downstream of the wind farm. The horizontal axis is longitude and the vertical axis is time. Figure 2b and c show time slices of the Hovmoller plot, illustrating the downstream development of the anomaly

patterns. When the wind farm is first turned off, the largest anomalies are located at the wind farm site. After five days have passed, the effect of the wind farm is most prominent in the North Atlantic, and the impacts reach the North Pacific after one week. The anomalies grow faster within the Atlantic and Pacific storm tracks than over land. After two weeks have elapsed, the perturbed run has largely diverged from the original run, obscuring the structure of the wind farm effects, although the largest anomalies are still found over the northern ocean basins.

Empirical orthogonal function (EOF) analysis was performed on each day post-disturbance, with case number as the primary dimension. The domain of the analysis focused on the region downstream of the wind farm. Four and a half days after the surface roughness change, the dominant EOF components display a wave-like structure located downstream of the wind farm, and extending into the North Atlantic (Fig. 3). The first two EOF components, which explain 22% of the total variability, are approximately in quadrature and depict a growing baroclinic mode. Although the magnitude of the first EOF component is small, the pattern is striking. Of the first ten EOF components, nine show varying downstream wave patterns. Cumulatively, these nine components account for 52% of the total variability, which indicates that the wind farm induces large instabilities in the downstream flow after a few days have elapsed from the roughness perturbation. A visual inspection of the zonal wind anomalies at 697 hPa over all of the case studies reveals a number of instances where a wave train occurs. Wave amplitude, wavelength, and channel width vary greatly across all of the cases, but each is confined to the central North Atlantic.

The case studies were also examined to find particularly large meteorological changes. In one case, a 40 m anomaly was observed in the 510 hPa geopotential height field four and a half days after the surface roughness change was triggered in the model. This is shown in Fig. 4a. The anomaly observed in this case exceeds the average error in a 5-day forecast of 500 hPa geopotential height over the North Atlantic, which is rarely larger than 20 m. We tested this result by restarting the case using five different sets of randomly perturbed initial conditions. The ensemble average and

standard deviation is presented in Fig. 4b. The structure and magnitude of the average anomaly is similar to the result shown in Fig. 4a. The standard deviation across the five ensemble members indicates that the ensemble error is small. The results of the ensemble imply that the induced perturbation persists through five different, randomly
5 perturbed tests.

4   Conclusions

The study presented here depicts a strong downstream impact caused by a large surface roughness perturbation in a GCM. The active control of turbine orientation would enable manipulation of the effective surface roughness of a wind farm. We have mod-
10 eled this as a time-dependent change in surface roughness. Atmospheric anomalies initially develop at the wind farm site due to a slowing of the obstructed wind. The anomalies propagate downstream as a variety of baroclinic and barotropic modes, and grow quickly when they reach the North Atlantic. These responses occur within a short forecast timeframe, which suggests that predictable influences on weather may be
15 possible. This study utilized an array of highly variable initial conditions to initialize the model. Ongoing work will catalog the initial meteorological conditions necessary to generate predictable and controlled downstream effects caused by wind farms. We performed an ensemble study of one particular case with randomly perturbed initial conditions chosen for both the wind farm and the wind farm absent cases that showed
20 that the atmospheric perturbation persists across the ensemble members. We will continue to study the wind farm effects in an ensemble context to determine the conditions necessary for induced perturbations to project strongly onto the fastest modes of error growth. This will illustrate the statistical significance and regularity of downstream changes in the atmosphere.

25 *Acknowledgements.* We thank Eugenia Kalnay for her comments and suggestions. We acknowledge Juliana Rew and Samuel Levis, at the National Center for Atmospheric Research

Weather response of a large wind turbine array

D. B. Barrie and
D. B. Kirk-Davidoff

Title Page

Abstract   Introduction

Conclusions   References

Tables   Figures

◄   ►►

◄   ►

Back   Close

Full Screen / Esc

Printer-friendly Version

Interactive Discussion

References

Archer, C. L. and Jacobson, M. Z.: Evaluation of global wind power. J. Geophys. Res., 110,
5   D12110, doi:10.1029/2004JD005462. 2005.

Aubrey, C., Pullen, A., Zervos, A., and Teske, S.: Global wind energy outlook 2006, Global Wind Energy Council (GWEC), Brussels, 2006.

Baidya Roy, S., Pacala, S. W., and Walko, R. L.: Can wind farms affect local meteorology?, J. Geophys. Res., 109, D19101, doi:10.1029/2004JD004763, 2004.

10   Barlage, M. and Zeng, X.: The effects of observed fractional vegetation cover on the land surface climatology of the community land model, J. Hydrometeorol., 5, 823–830, 2004.

Collins, W. D., Rasch, P. J., Boville, B. A., et al.: Description of the NCAR community atmosphere model (CAM 3.0), NCAR technical note, NCAR/TN-464+STR, 2004.

Collins, W. D., Bitz, C. M., Blackmon, M. L., et al.: The community climate system model version
15   3 (CCSM3), J. Climate, 19, 2122–2143, 2006.

Department of Energy: Wind Energy for Rural Economic Development, United States Department of Energy, Office of Energy Efficiency and Renewable Energy, Washington, DOE/GO-102004-1826, 2004.

Department of Energy: 20% wind energy by 2030 increasing wind energy's contribution to
20   the U. S. electricity supply, United States Department of Energy, Office of Energy Efficiency and Renewable Energy, Washington, DOE/GO-102008-2567, 2008.

Dorman, L. E., Khilji, N., Sastri, B., et al.: International Energy Outlook 2007, United States Department of Energy, Office of Integrated Analysis and Forecasting, Washington, DOE/EIA-0484(2007), 2007.

25   Elliott, D., Holladay, C. G., Barchet, W. R., Foote, H. P., and Sandusky, W. F.: Wind energy resource atlas of the United States, Department of Energy, DOE/CH 10093-4, 1986.

Hoffman, R. N.: Controlling the global weather, B. Am. Meteorol. Soc., 83, 241–248, 2002.

Hoffman, R. N., Henderson, J. M., Leidner, S. M., Grassotti, C., and Nehrkorn, T.: The response of damaging winds of a simulated tropical cyclone to finite-amplitude perturbations
30   of different variables, J. Atmos. Sci., 63, 1924–1937, 2006.

Weather response of a large wind turbine array

D. B. Barrie and
D. B. Kirk-Davidoff

Title Page

Abstract	Introduction
Conclusions	References
Tables	Figures

|◄ ►|

◄ ►

Back Close

Full Screen / Esc

Printer-friendly Version

Interactive Discussion

Kirk-Davidoff, D. B. and Keith, D.: On the climate impact of surface roughness anomalies, J. Atmos. Sci., 85, 2215–2234, doi:10.1175/2007JAS2509.1, 2008.

Kwa, C.: The rise and fall of weather modification: changes in American attitudes towards technology, nature, and society, Changing the Atmosphere: Expert Knowledge and Environmental Governance, 1st edn., edited by: C. Miller, The MIT Press, Cambridge, pp. 135–165, 2001.

Langmuir, I.: Control of precipitation from cumulus clouds by various seeding techniques, Science, 112, 35–41, 1950.

Lettau, H.: Note on aerodynamic roughness-parameter estimation on the basis of roughness-element description, J. Appl. Meteorol., 8, 828–832, 1969.

Lorenz, E. N.: Deterministic nonperiodic flow, J. Atmos. Sci., 20, 130–141, 1963.

Lorenz, E. N.: Atmospheric predictability as revealed by naturally occurring analogues, J. Atmos. Sci., 26, 636–646, 1969.

Macdonald, R. W., Griffiths, R. F., and Hall, D. J.: An improved method for the estimation of surface roughness of obstacle arrays, Atmos. Environ., 32, 1857–1864, 1998.

Medici, D.: Wind turbine wakes – control and vortex shedding, KTM Mechanics, Royal Institute of Technology, Stockholm, 2004.

Pacala, S. and Socolow, R.: Stabilization wedges: solving the climate problem for the next 50 years with current technologies, Science, 305, 968–972, 2004.

Schaefer, V. J.: The production of ice crystals in a cloud of supercooled water droplets, Science, 104, 457–459, 1946.

Schubert, S. D. and Suarez, M.: Dynamical predictability in a simple general circulation model: average error growth, J. Atmos. Sci., 46, 353–370, 1989.

Toth, Z. and Kalnay, E.: Ensemble forecasting at NMC: the generation of perturbations, B. Am. Meteorol. Soc., 74, 2317–2330, 1993.

Willoughby, H. E., Jorgensen, D. P., Black, R. A., and Rosenthal, S. L.: Project Stormfury: a scientific chronicle, B. Am. Meteorol. Soc., 66, 505–514, 1985.

Wiser, R. and Bolinger, M.: Annual report on U. S. wind power installation, cost, and performance trends: 2006, United States Department of Energy, Office of Energy Efficiency and Renewable Energy, Washington, DOE/GO-102007-2433, 2007.

Vermeer, L. J., Sorensen, J. N., and Crespo, A.: Wind turbine wake aerodynamics, Prog. Aerosp. Sci., 39, 467–510, 2003.

Weather response of a large wind turbine array

D. B. Barrie and
D. B. Kirk-Davidoff

Title Page

Abstract | Introduction

Conclusions | References

Tables | Figures

⏮ | ⏭

◀ | ▶

Back | Close

Full Screen / Esc

Printer-friendly Version
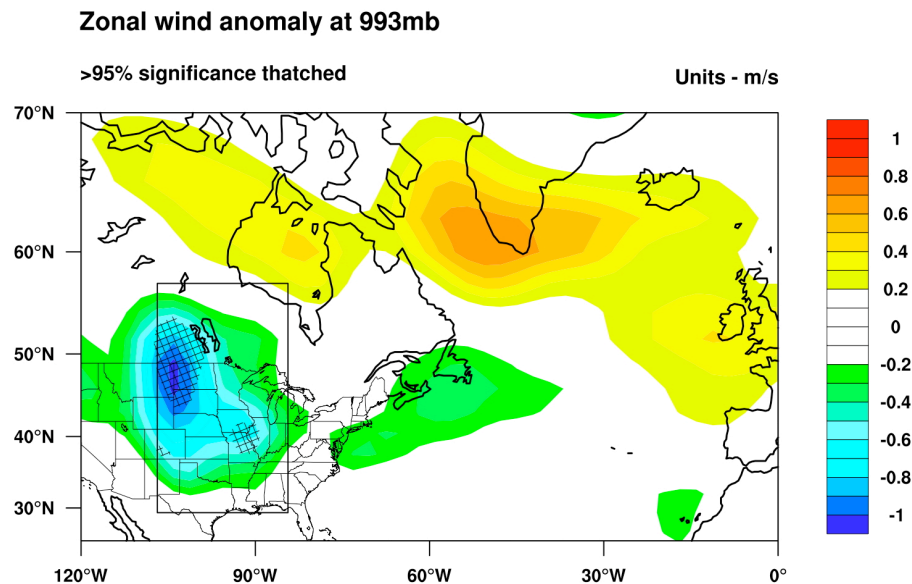
Interactive Discussion

Fig. 1. 993 mbar zonal wind anomaly. The mean difference in the eastward wind in the lowest model level between the control and perturbed model runs highlights regions of atmospheric modification. Regions where significance exceeds 95%, as determined by a Student's t-test, are thatched. The wind farm is located within the rectangular box over the central United States and central Canada. Areas of the wind farm located over water are masked out during the model runs.
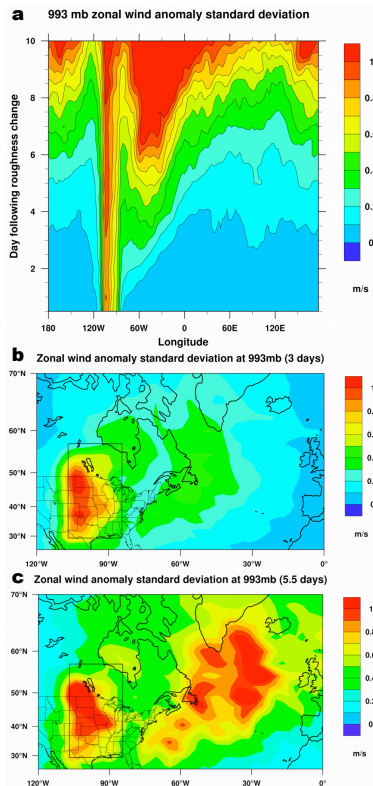
Fig. 2. Growth and propagation of anomalies. **(a)** A Hovmoller plot shows the standard deviation of anomalies versus forecast lead time and longitude, highlighting the growth rate and group velocity of perturbations. **(b)** The standard deviation over all cases of the anomalous lower tropospheric zonal wind field one half day after the roughness change is depicted. This plot is equivalent to a time slice of panel a at time day=3. The largest effects are confined to the wind farm. **(c)** Same as panel **(b)** except at time day=5.5. The largest effects are now located over the North Atlantic.

Weather response of a large wind turbine array

D. B. Barrie and
D. B. Kirk-Davidoff

Title Page

Abstract | Introduction

Conclusions | References

Tables | Figures

◄ | ►►

◄ | ►

Back | Close

Full Screen / Esc

Printer-friendly Version

Interactive Discussion

EOF of day 4 geopotential height at 697 mb
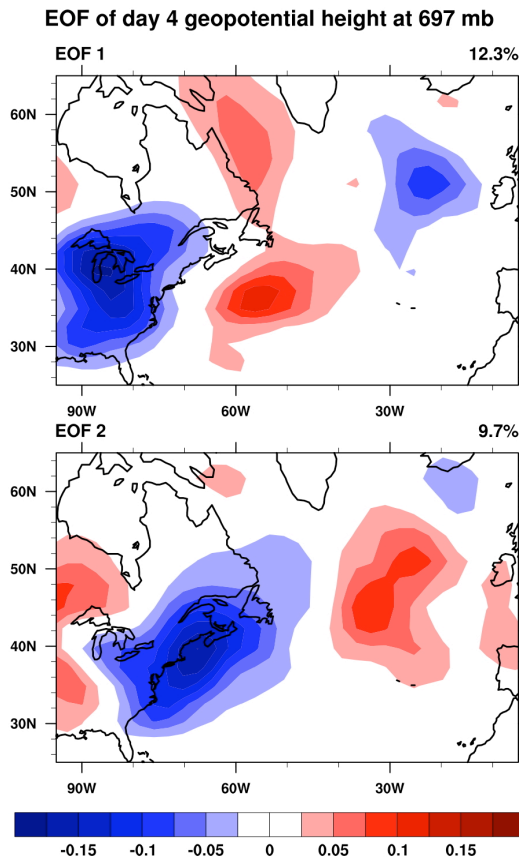
Fig. 3. EOF analysis of day four 697 mbar zonal wind. The first two components of an EOF analysis are displayed. They depict the two largest modes of variability associated with the surface roughness perturbation.

Weather response of a large wind turbine array

D. B. Barrie and
D. B. Kirk-Davidoff

a   **Geopotential height anomaly at 510mb (4.5 days)**

b   **Ensemble average geopotential height anomaly at 510mb (4.5 days)**

Standard deviation across ensemble members is contoured
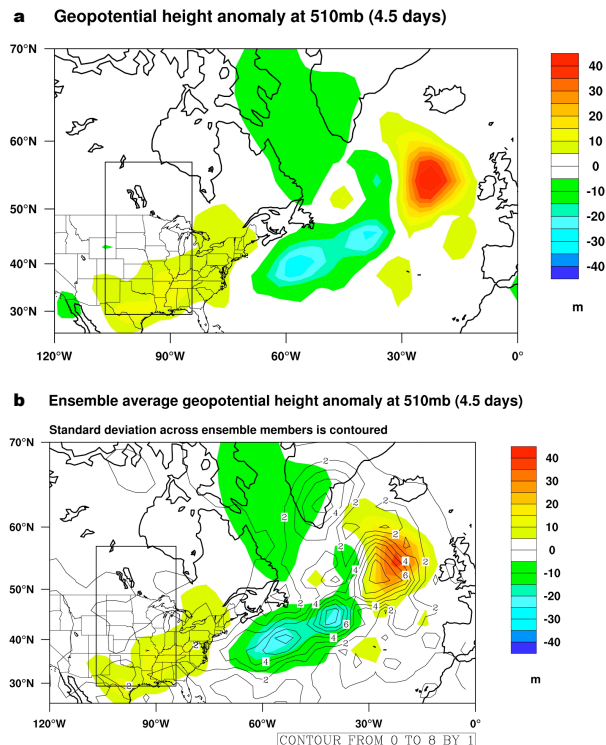
CONTOUR FROM 0 TO 8 BY 1

Fig. 4. 510 mbar geopotential height. These plots of geopotential height depict a particular case where a large modification of weather occurred four and a half days after the surface roughness modification. **(a)** The anomaly field (calculated as the difference between the case with the wind farm on, and the case with it off) shows changes in geopotential height of approximately 40 m. **(b)** The results of an ensemble study of the case depicted in Fig. 4a is shown. The average anomalies are shaded, and the standard deviation across the ensemble components is shown in contours.